Hindawi
Advances in Civil Engineering
Volume 2019, Article ID 8963971, 7 pages
https://doi.org/10.1155/2019/8963971

Research Article

Influence of Particle Size Distribution on the Critical State of Rockfill

Gui Yang,[1] **Yang Jiang**,[1] **Sanjay Nimbalkar**,[2] **Yifei Sun**,[1] **and Nenghui Li**[3]

[1]*Key Laboratory of Ministry of Education for Geomechanics and Embankment Engineering, College of Civil and Transportation Engineering, Hohai University, Nanjing 210098, China*
[2]*School of Civil and Environmental Engineering, Faculty of Engineering and Information Technology, University of Technology, Sydney, NSW 2007, Australia*
[3]*Nanjing Hydraulic Research Institute, Nanjing 210024, China*

Correspondence should be addressed to Gui Yang; ygheitu@163.com

Received 24 June 2019; Revised 20 August 2019; Accepted 17 September 2019; Published 20 October 2019

Academic Editor: Chun-Qing Li

In order to study the effect of particle size distribution on the critical state of rockfill, a series of large-scale triaxial tests on rockfill with different maximum particle sizes were performed. It was observed that the intercept and gradient of the critical state line in the $e - p'$ plane decreased as the grading broadened with the increase in particle size while the gradient of the critical state line in the $p' - q$ plane increased as the particle size increased. A power law function is found to appropriately describe the relationship between the critical state parameters and maximum particle size of rockfill.

1. Introduction

The construction of earthfill and rockfill dams has given new impetus to investigation of the physical and mechanical properties of rockfill material [1]. In most cases, triaxial testing on the prototype rockfill using conventional laboratory equipment is unattainable as the sizes of aggregates used in the field are usually too large. This in turn emphasizes the need to develop appropriate scaling laws. However, the strength of rockfill is greatly influenced by the size distribution of the crushed stone aggregates. Results of triaxial tests on rockfill reported by Marachi et al. [2] revealed that the friction angle increased with the decrease in maximum particle size (d_{M}). On the contrary, different trends were observed from the results of direct shear tests on glass beads [3] and triaxial tests on ballast [4]. Another important governing factor for the design of the hydraulic dam is the critical state behaviour of constituting rockfill aggregates [5, 6]. In these studies, the critical state line proposed by Li and Wang [7] was used to evaluate the effect of particle size distribution on the critical state of granular aggregates. Through discrete element modelling of granular aggregates, the critical state stress ratio (M_{cs}) was found to be insensitive to any change in the coefficient of uniformity (C_{u}), but the critical state parameters (e_{cs0}, λ_{s}) in the $e - (p'/p_{\mathrm{a}})^{\xi}$ plane decreased with the increase in C_{u} [8, 9]. However, the effect of d_{M} on the critical state of granular soil is still largely unknown. The parallel gradation and combination methods [10] are widely acknowledged in testing and designing of rockfill, inevitably instigating the use of reduced d_{M}.

The purpose of this study is to investigate the influence of particle size distribution (PSD) adopting the combination method on the critical state of rockfill. Therefore, a series of monotonic drained tests using a large-scale triaxial apparatus were performed on graded rockfill materials with varying d_{M}. Based on laboratory findings, a general relationship between the critical state parameters and d_{M} is proposed.

2. Laboratory Testing

2.1. Test Material. The rockfill material used in this study was collected from the Xiaolangdi Dam in Jiyuan, Henan

Province of China. Aggregates were derived from the parent sandstone rock. Visual inspection revealed that aggregates larger than 5 mm in size had a rounded/subrounded shape. The finer fraction (size less than 5 mm) contained sand-gravel particles. Based on the values of coefficient of uniformity and coefficient of curvature ($C_u = 90$, $C_c = 1.7$), rockfill was classified as well graded [11]. The prototype grading ($d_M = 250$ mm) and the corresponding four scaled down PSDs of Xiaolangdi rockfill via the method of combination are shown in Figure 1. The d_M of each grading are 40 mm (T4), 60 mm (T3), 80 mm (T2), and 120 mm (T1), respectively. In tests, the different grading specimens are compacted with the same relative density 0.90. The sample diameter (Φ) and density (ρ) are also listed in Figure 1.

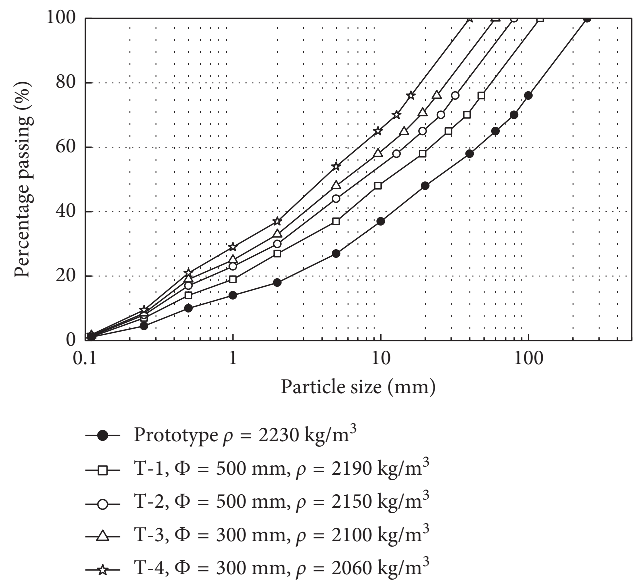

Figure 1: Prototype and initial gradings of Xiaolangdi rockfill.

2.2. Test Procedure. A large-scale triaxial apparatus designed and built in Nanjing Hydraulic Research Institute was used. The maximum cell pressure is 4.0 MPa, maximum axial loading force is 5000 kN, and maximum axial displacement is 250 mm. The apparatus can accommodate samples of different diameters (Φ), such as $\Phi = 500$, 300, and 200 mm. Particles selected from each size range were carefully washed and dried under natural sunlight. Subsequently, aggregates were weighed separately and mixed together before splitting into either sixteen equal portions (to prepare the test specimen with 500 mm in diameter and 1100 mm in height) or ten equal portions (to form the test specimen with a diameter of 300 mm and a height of 700 mm). Each portion was then compacted inside a split cylindrical mould using a vibrator (as shown in Figure 2). The motor power is 1.2 kW ($\Phi = 300$ mm) and 1.8 kW ($\Phi = 500$ mm), respectively. Each portion was compacted for 60 s ($\Phi = 300$ mm) and 90 s ($\Phi = 500$ mm), respectively. According to the study's results [12], the influence of different sample diameter sizes can be ignored. During vibratory compaction, a static pressure of 14 kPa and a frequency of 20 Hz were applied to achieve desired initial density simulating in-field conditions. The test specimen was then placed inside a test chamber. Before commencement of the monotonic shear test, the sample was saturated by allowing water to pass through the base of the triaxial cell under a back pressure of 10 kPa until Skempton's B-value exceeded 0.95. The samples were then isotropically consolidated at effective confining pressures (σ_3') of 0.2–2.2 MPa before monotonic loading. Triaxial tests were then conducted under the monotonic drained condition with a constant axial displacement rate of 2.7 mm/min until the axial strain was accumulated up to 15%.

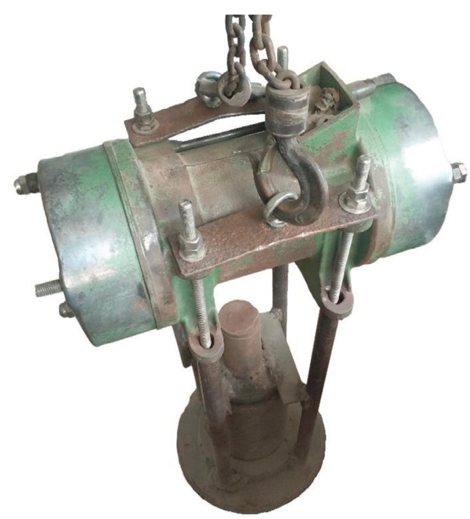

Figure 2: Vibration equipment.

3. Result Analysis

3.1. Stress-Strain Behaviour. The stress-strain behaviour of Xiaolangdi rockfill tested at varying maximum particle sizes (d_M) of 40, 60, 80, and 120 mm are shown in Figures 3–6, respectively. Different values of initial confining pressure (σ_3') such as 0.2, 0.4, 0.8, 1.6, and 2.2 MPa were chosen. Specimen tested at low pressure ($\sigma_3' = 0.2$ MPa, $d_M = 120$ mm) exhibited mild strain-softening behaviour and dilatancy. On the contrary, prominent strain-hardening behaviour and contraction [13, 14] were also observed in the specimen tested under higher σ_3' (>0.2 MPa). The volumetric strain decreased with the increase in d_M while the axial strain increased with decrease in d_M at the same stress level. Moreover, with the increase of d_M, the peak shear strength of rockfill (σ_f) was improved (for example, $\sigma_f = 3.10$, 3.14, 3.27, and 3.44 MPa corresponding to $\sigma_3' = 0.8$ MPa). This finding is contrary to that reported by Marachi et al. [2] where an improved strength was associated with the reduced d_M of the (angular) rockfill aggregates. This was probably due to the different aggregate shapes used in this study (rounded/subrounded and flaky) which had influenced the frictional interlock and breakage of aggregates. More discussion on these aspects is given by Varadarajan et al. [15] and Dai et al. [3].

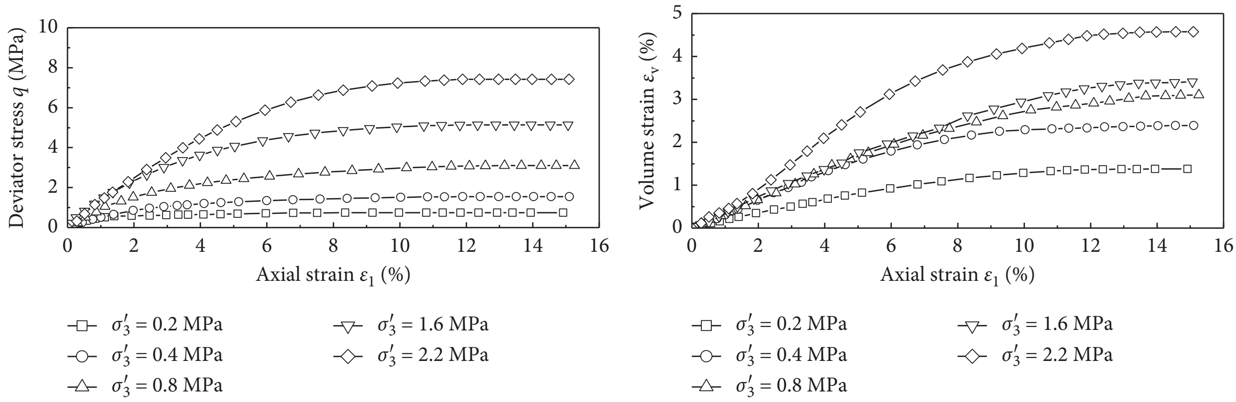

(a) (b)

FIGURE 3: Stress-strain behaviors of rockfill with $d_M = 40$ mm.

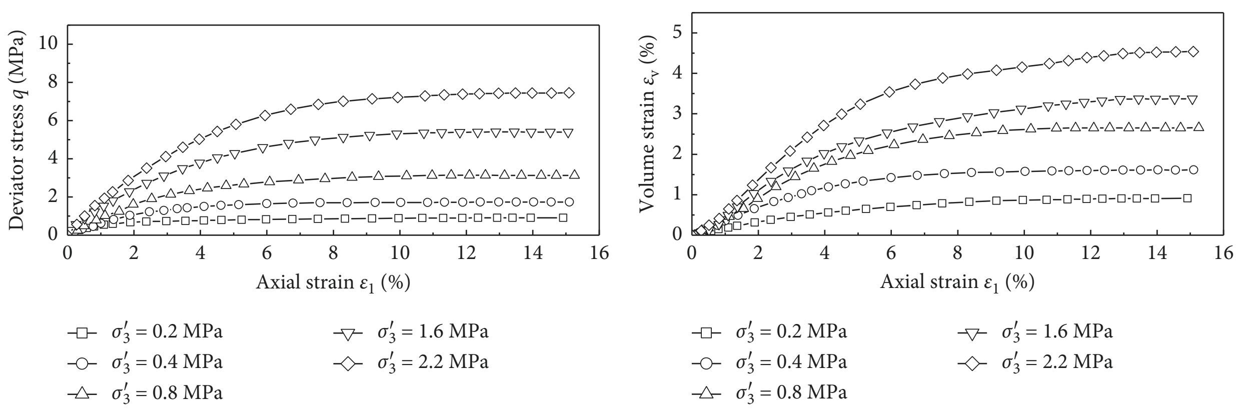

(a) (b)

FIGURE 4: Stress-strain behaviors of rockfill with $d_M = 60$ mm.

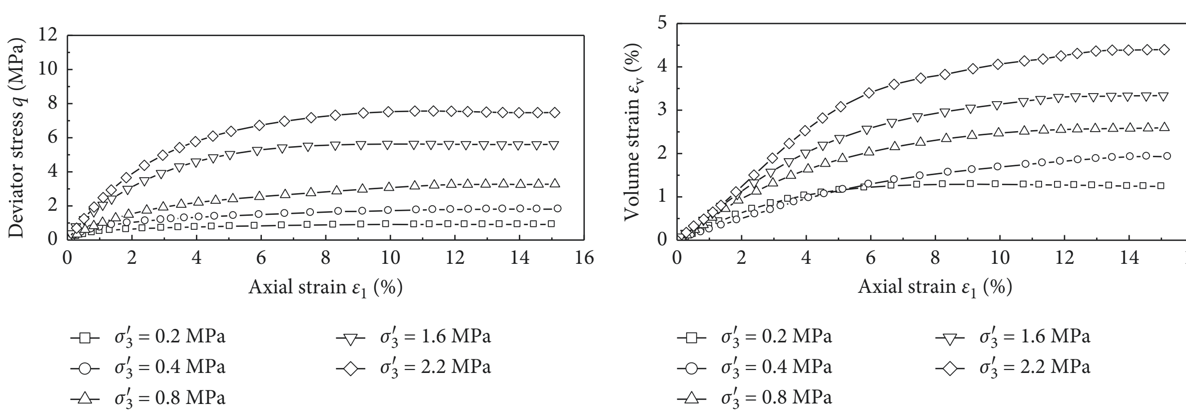

(a) (b)

FIGURE 5: Stress-strain-volume behaviors of rockfill with $d_M = 80$ mm.

3.2. Critical State Strength. Critical state of rockfill is the core concept in elastoplastic constitutive modelling [16]. As evident from the laboratory data, the deviator stress and volumetric strain became almost stabilized at the end of each test; therefore, the critical state of each rockfill specimen could be obtained by measuring the final state of shearing (Figures 3–6). The critical state line is plotted in the $p' - q$ plane as shown in Figure 7. It could be

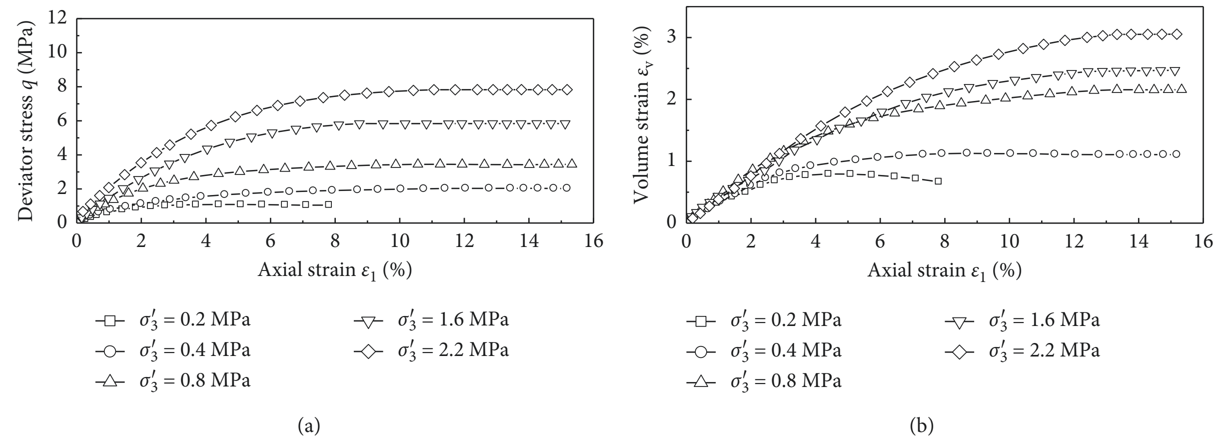

Figure 6: Stress-strain-volume behaviors of rockfill with $d_M = 120$ mm.

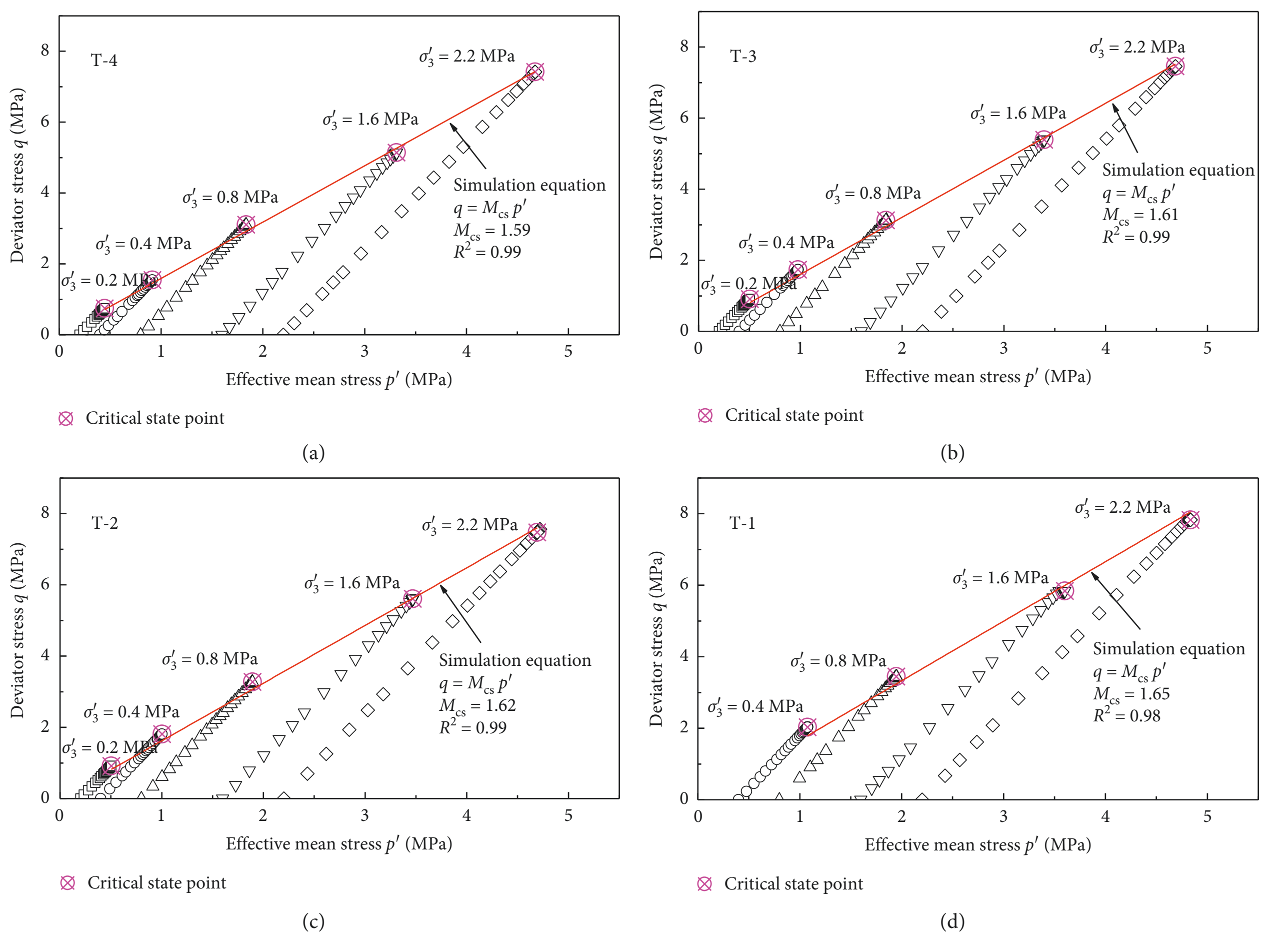

Figure 7: (a) Critical state line in the $p' - q$ plane for rockfill with $d_M = 40$ mm. (b) Critical state line in the $p' - q$ plane for rockfill with $d_M = 60$ mm. (c) Critical state line in the $p' - q$ plane for rockfill with $d_M = 80$ mm. (d) Critical state line in the $p' - q$ plane for rockfill with $d_M = 120$ mm.

concluded that the critical state stress ratio ($M_{cs} = q/p'$) is constant for a given PSD. However, unlike past published studies which reported independency of M_{cs} with C_u [8, 9], M_{cs} was found to increase as d_M increased in this study (Figure 8). This dependency of M_{cs} with d_M could be described by adopting the power law relationship given below:

$$M_{cs} = a_1 \left(\frac{d_M}{d_n} \right)^{b_1}, \tag{1}$$

where d_n is equal to 60 mm (nominal particle diameter chosen arbitrarily for the purpose of normalization) and a_1 and b_1 are material constants, equal to 1.61 and 0.0332, respectively.

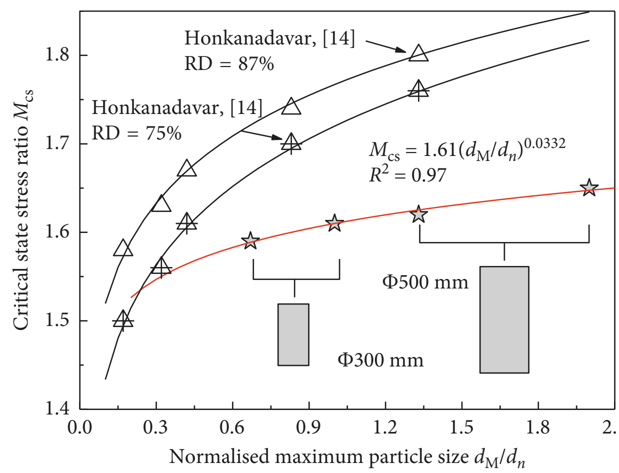

Figure 8: Variation of critical state stress ratio with particle size.

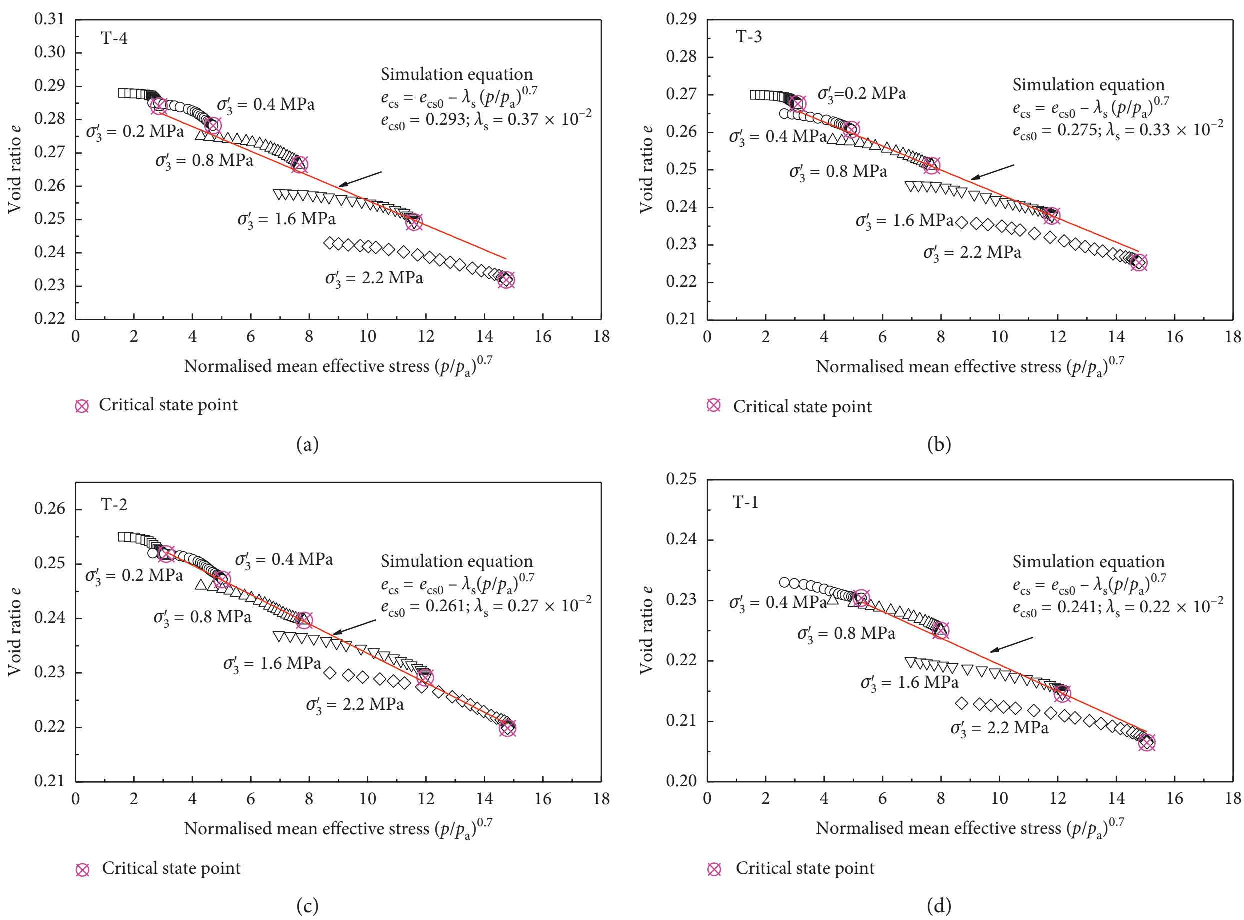

Figure 9: (a) Critical state line in the $e - (p'/p_a)^{0.7}$ plane for rockfill with $d_M = 40$ mm. (b) Critical state line in the $e - (p'/p_a)^{0.7}$ plane for rockfill with $d_M = 60$ mm. (c) Critical state line in the $e - (p'/p_a)^{0.7}$ plane for rockfill with $d_M = 80$ mm. (d) Critical state line in the $e - (p'/p_a)^{0.7}$ plane for rockfill with $d_M = 120$ mm.

This is similar to the test results of Honkanadavar and Sharma [14]. M_{cs} is calculated according to internal friction angle φ (related to the critical state value $M_{cs} = 6 \sin\varphi/(3 - \sin\varphi)$).

The critical state line of granular aggregates in the $e - \ln p'$ plane may shift or rotate with increasing loading stress due to particle degradation [17, 18]. Therefore, the nonlinear critical state line proposed by [7] is used:

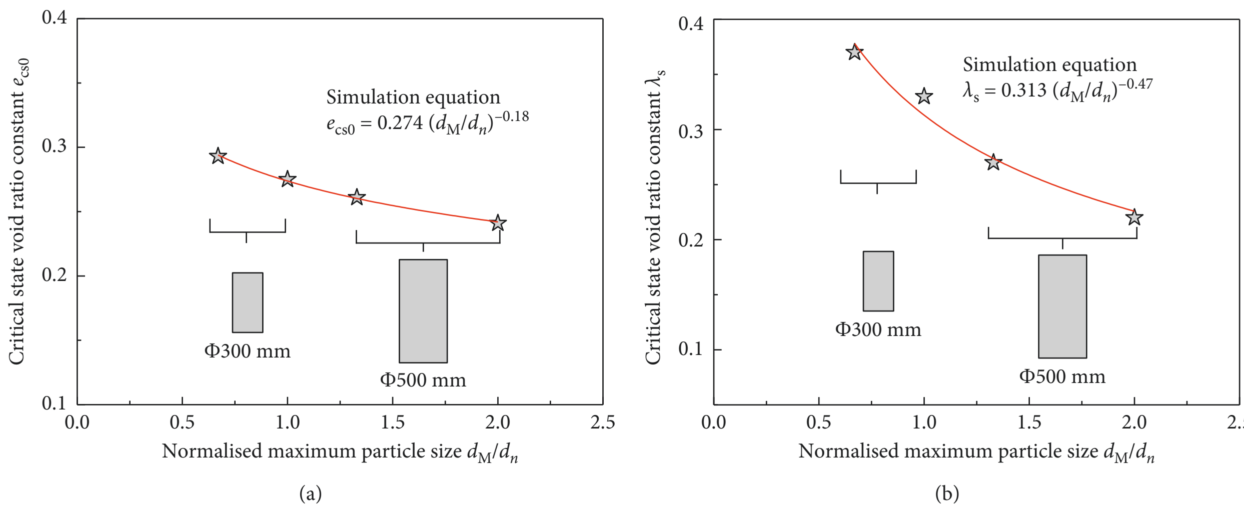

FIGURE 10: (a) Variation of e_{cs0} with particle size. (b) Variation of λ_s with particle size.

$$e_{cs} = e_{cs0} - \lambda_s \left(\frac{p'}{p_a}\right)^{\xi}, \tag{2}$$

where e_{cs} denotes the critical state void ratio; e_{cs0} and λ_s are dimensionless material constants; and $p_a = 101$ kPa is the atmospheric pressure used for the purpose of normalization. The parameter $\xi = 0.7$ is used in this study which shows good resemblance with laboratory data. Figure 9 shows the critical state lines along with the critical state stress points of Xiaolangdi rockfill with differing d_M. A linear correlation between e_{cs} and $(p'/p_a)^{\xi}$ could be observed. With the increase of d_M, e_{cs} was found to decrease. The influence of d_M on the critical state line (equation (2)) is indicated by the variation of the gradients and intercepts of samples with different gradings. As evident from Figure 10, both e_{cs0} and λ_s showed decrease with the increase in d_M, which can be described by the following power law relationships:

$$\begin{aligned} e_{cs0} &= a_2 \left(\frac{d_M}{d_n}\right)^{b_2}, \\ \lambda_s &= a_3 \left(\frac{d_M}{d_n}\right)^{b_3}, \end{aligned} \tag{3}$$

where a_2, a_3, b_2, and b_3 are material constants, equal to 0.274, −0.18, 0.313, and −0.47, respectively. This simple empirical relationship could be introduced into an elastoplastic model [19, 20] developed within the framework of critical-state soil mechanics to simulate the stress-strain behaviour of rockfill more appropriately.

4. Conclusions

Critical state strength of granular aggregates, including rockfill, is an important aspect for constitutive modelling. However, due to the limitation of conventional laboratory equipment, the critical state behaviour of field rockfill is usually obtained by scaling down aggregate sizes. This in turn can lead to inaccuracies in prediction of material performance in "in situ" conditions. In this study, the influence of particle size distribution on the critical state strength of rockfill was investigated by adopting the combination method. A series of drained large-scale triaxial tests were performed on rockfill materials procured from the Xiaolangdi dam. Stress-strain analysis was performed on the test specimen with four different maximum particle sizes (i.e., $d_M = 40$, 60, 80, and 120 mm) and five different initial confining pressures (i.e., $\sigma_3' = 0.2$, 0.4, 0.8, 1.6, 2.2 MPa). The major findings of this study are summarized below:

(a) The volumetric strain decreased with the increase in d_M while the axial strain increased with a decrease in d_M, at the same stress level. With the increase of d_M, the peak shear strength of rockfill was observed to improve.

(b) The critical state lines in both $p' - q$ and $e - p'$ planes were influenced by the particle sizes. The critical state stress ratio (M_{cs}) increased with an increase in d_M while the gradient (λ_s) and intercept (e_{cs}) decreased as d_M increased.

(c) Based on the laboratory data presented in this study, a power law relationship was proposed for describing the evolution of the critical state parameters with d_M. This simple yet accurate empirical relationship could be introduced into a critical-state constitutive model to simulate the stress-strain behaviour of rockfill under a range of particle sizes. This empirical relationship is based on the limited test data and it needs further validation for a wider range of particle sizes.

Data Availability

The data used to support the findings of this study are available from the corresponding author upon request.

Conflicts of Interest

The authors declare that they have no conflicts of interest.

Acknowledgments

The financial support provided by the National Natural Science Foundation of China (no. 51479059) and Fundamental Research Funds for the Central Universities of China (no. 2017B12514) is greatly appreciated.

References

[1] R. J. Marsal, "Large scale testing of rockfill materials," *Journal of the Soil Mechanics and Foundations Division*, vol. 93, no. 2, pp. 27–43, 1967.

[2] N. D. Marachi, C. K. Chan, and H. B. Seed, "Evaluation of properties of rockfill materials," *Journal of the Soil Mechanics and Foundations Division*, vol. 98, no. 1, pp. 95–114, 1972.

[3] B. Dai, J. Yang, and C. Zhou, "Observed effects of interparticle friction and particle size on shear behavior of granular materials," *International Journal of Geomechanics*, vol. 16, no. 1, Article ID 04015011, 2016.

[4] B. Indraratna, Y. Sun, and S. Nimbalkar, "Laboratory assessment of the role of particle size distribution on the deformation and degradation of ballast under cyclic loading," *Journal of Geotechnical and Geoenvironmental Engineering*, vol. 142, no. 7, Article ID 04016016, 2016.

[5] Y. Xiao, H. Liu, Y. Chen, and J. Jiang, "Strength and deformation of rockfill material based on large-scale triaxial compression tests. I: influences of density and pressure," *Journal of Geotechnical and Geoenvironmental Engineering*, vol. 140, no. 12, Article ID 04014070, 2014.

[6] C. Ovalle, E. Frossard, C. Dano, W. Hu, S. Maiolino, and P.-Y. Hicher, "The effect of size on the strength of coarse rock aggregates and large rockfill samples through experimental data," *Acta Mechanica*, vol. 225, no. 8, pp. 2199–2216, 2014.

[7] X. S. Li and Y. Wang, "Linear representation of steady-state line for sand," *Journal of Geotechnical and Geoenvironmental Engineering*, vol. 124, no. 12, pp. 1215–1217, 1998.

[8] G. Li, Y. Liu, C. Dano, and P. Hicher, "Grading-dependent behavior of granular materials: from discrete to continuous modeling," *Journal of Engineering Mechanics*, vol. 141, no. 6, Article ID 04014172,, 2015.

[9] W. M. Yan and J. Dong, "Effect of particle grading on the response of an idealized granular assemblage," *International Journal of Geomechanics*, vol. 11, no. 4, pp. 276–285, 2011.

[10] K. Wei, S. Zhu, and X. Yu, "Influence of the scale effect on the mechanical parameters of coarse-grained soils," *IJST-Transactions of Civil Engineering*, vol. 38, no. C1, pp. 75–84, 2014.

[11] ASTM C1252, *Standard Test Methods for Uncompacted Void Content of Fine Aggregate (As Influenced by Particle Shape, Surface Texture, and Grading)*, ASTM International, West Conshohocken, PA, USA, 2006.

[12] R. Wen, C. Tan, Y. Wu, and C. Wang, "Grain size effect on the mechanical behavior of cohesionless coarse-grained soils with the discrete element method," *Advances in Civil Engineering*, vol. 2018, Article ID 4608930, 6 pages, 2018.

[13] Y. Xiao, H. Liu, Y. Chen, J. Jiang, and W. Zhang, "Testing and modeling of the state-dependent behaviors of rockfill material," *Computers and Geotechnics*, vol. 61, pp. 153–165, 2014.

[14] N. P. Honkanadavar and K. G. Sharma, "Testing and modeling the behavior of riverbed and blasted quarried rockfill materials," *International Journal of Geomechanics*, vol. 14, no. 6, Article ID 04014028, 2014.

[15] A. Varadarajan, K. G. Sharma, K. Venkatachalam, and A. K. Gupta, "Testing and modeling two rockfill materials," *Journal of Geotechnical and Geoenvironmental Engineering*, vol. 129, no. 3, pp. 206–218, 2003.

[16] Y. Xiao and H. Liu, "Elastoplastic constitutive model for rockfill materials considering particle breakage," *International Journal of Geomechanics*, vol. 17, no. 1, Article ID 04016041, 2017.

[17] V. Bandini and M. R. Coop, "The influence of particle breakage on the location of the critical state line of sands," *Soils and Foundations*, vol. 51, no. 4, pp. 591–600, 2011.

[18] A. R. Russell and N. Khalili, "A bounding surface plasticity model for sands exhibiting particle crushing," *Canadian Geotechnical Journal*, vol. 41, no. 6, pp. 1179–1192, 2004.

[19] L. A. Oldecop and E. E. Alonso, "A model for rockfill compressibility," *Géotechnique*, vol. 51, no. 2, pp. 127–139, 2001.

[20] M. Liu, Y. Gao, and H. Liu, "An elastoplastic constitutive model for rockfills incorporating energy dissipation of nonlinear friction and particle breakage," *International Journal for Numerical and Analytical Methods in Geomechanics*, vol. 38, no. 9, pp. 935–960, 2014.